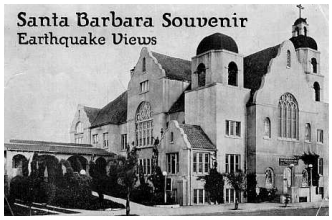

4th IASPEI / IAEE International Symposium:

Effects of Surface Geology on Seismic Motion

August 23–26, 2011 · University of California Santa Barbara

TESTING SCEC 3D SEISMIC VELOCITY MODELS FOR THE LOS ANGELES BASIN REGION

Robert W. Graves
US Geological Survey
Pasadena, CA, 91106
USA

ABSTRACT

The 2001 M_w 4.6 Big Bear Lake earthquake was recorded at over 180 broadband sites of the Southern California Seismic Network throughout the greater Los Angeles region of southern California. For frequencies less than about 1 Hz, the ground motions in the San Bernardino, San Gabriel and Los Angeles basins have significantly larger amplitudes and extended durations relative to sites outside the basins. This study extends previous analyses by modeling the motions using two Southern California Earthquake Center three-dimensional seismic velocity models (CVM-S4 and CVM-H11.1.0). The CVM-S4 simulations generally perform better than CVM-H11.1.0 at reproducing the observed waveforms, amplitudes, and durations, especially in the San Bernardino and San Gabriel basins at frequencies of 0.3 Hz and less. At higher frequencies (0.5 – 1.0 Hz), the fit to the recorded motions is less well resolved for both models. This reinforces the conclusions of Graves (2008) that deterministic modeling at frequencies approaching 1 Hz in regions of complex geology involves more than simply reducing the minimum velocity threshold, but also requires knowledge of the subsurface structure and distribution of seismic velocities at relatively short length scales.

INTRODUCTION

Analysis of the shorter period (around 1 sec) basin response in the San Bernardino region was first performed by Frankel (1994) using aftershocks of the 1992 Landers / Big Bear earthquake sequence recorded on temporary instrument arrays. The data were obtained on three tripartite arrays, two situated on the basin sediments and one on a nearby rock site. He found significant amplification of motions and much longer durations of shaking at the basin sites relative to the rock site. In addition, array analysis of the waveform data showed that the later-arriving phases are dominated by surface waves propagating in various directions across the basin. Using a relatively simple 3D velocity model, he was able to reproduce the general characteristics of these data. The main limitations of the Frankel (1994) study were that the instrument arrays only sampled the basin response at two locations, the bandwidth of the recordings was restricted due to the instrumentation and small event magnitudes ($M < 3$), and the small magnitudes precluded determination of robust source mechanism information.

Graves (2008) built on this previous work in the San Bernardino basin region through the analysis and 3D simulation of ground motion data from the 2001 M_w 4.63 Big Bear Lake earthquake. This event was recorded at numerous digital strong motion and broadband instrument sites, including about 20 sites within the San Bernardino basin. The magnitude of this event is large enough to generate significant energy at the mid-period range (1-5 seconds), yet small enough so that source process is relatively simple in this bandwidth. These characteristics allow for a more detailed analysis of the ground motion response than was possible in the earlier studies. The San Bernardino basin 3D seismic velocity model developed by Graves (2008) is based on the basement surface model proposed by Anderson et al. (2000). This model is characterized by a gently southwestward dipping basement interface that reaches its maximum depth just north of the San Jacinto fault. The Graves (2008) model does well at reproducing the waveforms, amplitudes and duration of the recorded motions in the frequency range of $f < 0.3$ Hz. At higher frequencies (approaching 1 Hz) the amplification and duration characteristics of the motions are matched well, although the deterministic fit to the waveforms is less well resolved.

In the current work, I extend these previous studies by considering additional 3D seismic velocity models that have been developed for the southern California region by the Southern California Earthquake Center (SCEC). These models are the SCEC Community Velocity Model (CVM) version 4 (Magistrale et al., 2000; Kohler et al., 2003; hereafter referred to as CVM-S4) and version 11.1.0 of the SCEC CVM-Harvard (Suess and Shaw, 2003; Tape et al., 2009; hereafter referred to as CVM-H11.1.0). In addition, I have extended the simulations for these models to include sites across the San Gabriel, San Fernando and Los Angeles basin regions.

In the sections that follow, I first discuss the characteristics of the observed ground motions for this event in the San Bernardino basin region. I then provide a review of the available 3D seismic velocity models, including comparisons of the SCEC models with the Graves (2008) model. This is followed by a detailed discussion of the ground motion simulations for the Big Bear Lake earthquake, along with a comprehensive comparison of the synthetic and recorded waveforms at both basin and non-basin sites. I conclude with a discussion of the factors that are currently limiting our ability to deterministically model the recorded waveforms at shorter periods, as well as recommendations for future improvements to the seismic velocity models.

OBSERVED GROUND MOTIONS

The M_w 4.63 Big Bear Lake earthquake occurred on 02/10/01 at a depth of 7.5 km just north of the San Bernardino region of southern California. The mechanism of the event is primarily strike-slip (Table 1) as determined by regional waveform inversion (e.g., Zhu and Helmberger, 1996). Ground motion waveforms were recorded at nearly 180 stations throughout the southern California region. These stations are part of the Southern California Seismic Network (SCSN) operated jointly by the US Geological Survey (USGS) and Caltech, and the California Strong Motion Instrumentation Program (CSMIP) operated by the California Geological Survey (CGS). The waveform data are available from the SECEC Data Center (http://www.data.scec.org) and the Center for Engineering Strong Motion Data (http://www.strongmotioncenter.org). Figure 1 shows the distribution of the recording stations and the event epicenter. Note that there is a large concentration of stations within the San Bernardino basin, which lies in the wedge shaped region between the San Andreas and San Jacinto faults.

Table 1. Source parameters.

Date	02/10/01
Origin Time	21:05:05.34
Latitude	34.2913
Longitude	-116.9403
Moment	1×10^{23} dyne-cm
Depth	7.5 km
Strike	208^o
Dip	77^o
Rake	10^o

From these data, I have extracted peak ground velocity (PGV) from the waveforms for different frequency bandwidths. Here, I define PGV as the largest peak amplitude of the three recorded components at each site. Figure 1 shows maps of the contoured PGV values for data filtered at $f < 0.3$ Hz and $f < 1.0$ Hz. These maps show noticeable amplification to the southwest of the epicenter in the San Bernardino basin, as well as further to the west in the Los Angeles and San Fernando basins. In particular, there is a strong peak in the amplification pattern along the northeastern margin of the Los Angeles basin near its juncture with the San Gabriel basin (around lon=-118^o, lat=34^o).

Figure 2 shows a map view of the stations in the San Bernardino region along with profiles of the recorded ground motion time histories rotated to tangential and radial components relative to the epicenter. For these profiles, I have integrated the recorded accelerations to ground velocity. The waveforms in these profiles are filtered in the passband $f < 1.0$ Hz. The plotting sequence of the stations in these profiles is roughly with increasing epicentral distance. Thus, the stations at the top of the profiles are located closest to the epicenter, generally along the northern margin of the San Bernardino basin, the stations in the middle of the profiles are located within the central basin (indicated by the red brackets), and the stations at the bottom of the profiles are located furthest from the epicenter, generally south and west of the basin.

The motions at the sites along the northern margin of the basin are characterized by relatively short durations (less than about 5 sec) with the peak motions primarily being controlled by the direct S wave. Although these sites are located outside of the deep basin

region (i.e., non-basin sites), there is still some complexity and variability in the observed waveforms.

The stations located within the central basin region clearly show amplified motions and extended durations of shaking relative to the sites outside of the basin. In addition, for many of the basin sites the largest motions occur later in the records after the direct arrivals. This is particularly apparent for the lower frequency motions, suggesting the influence of deeper geologic structure as opposed to near-surface site response effects. These types of ground motion characteristics are indicative of basin response effects such as the generation and propagation of basin surface waves.

The motions at stations south and west of the basin (e.g., **np5330**, **FON**, **RVR**) have noticeably lower amplitudes than the nearby basin sites. This is particularly true for the later arriving phases. In many respects, the motions at these sites are much more similar to the motions at sites north of the basin than they are to sites within the basin itself. This suggests that the influence of the basin structure is primarily limited to those sites located in the central basin region, and that the basin generated waves do not "leak" out of the basin in a significant manner.

3D VELOCITY STRUCTURE IN THE SAN BERNARDINO REGION

The San Bernardino region of southern California is situated on a wedge-shaped sedimentary basin bounded to the north by the San Andreas fault and to the south by the San Jacinto fault. The shape of the bedrock surface underlying the basin sediments has been determined from the analysis of potential field data (Anderson et al., 2000). The basin depth is quite shallow along the San Andreas fault and increases towards the southwest, reaching a maximum of about 1800 m just north of the San Jacinto fault. Southwest of this point, the basement surface steps up abruptly and has an average depth of about 300 m in the Fontana/Chino basin west of the fault.

In the previous study of the Big Bear Lake earthquake, Graves (2008) developed a 3D velocity structure using this basement surface. That study used a minimum shear wave velocity of 250 m/s in the basin and the modeling bandwidth was restricted to frequencies of 1 Hz and less. This minimum shear wave velocity is consistent with a class D site type, which has an expected V_{s30} value in the range of 180 m/s to 360 m/s (Wills et al., 2000). Most of the sites in the San Bernardino basin are class CD or D (Wills et al., 2000). Additionally, Graves (2008) added a gradient in the near surface of the media outside the basin, which lowers the surface shear wave velocity to 700 m/s. This is consistent with a class B site type (Wills et al., 2000).

For the current simulations, we consider two additional 3D seismic velocity models. The first model, CVM-S4, is the SCEC CVM-4.0 (Magistrale et al., 2000; Kohler et al., 2003) (http://www.data.scec.org/3Dvelocity). The second model, CVM-H11.1.0, is version 11.1.0 of the SCEC CVM-H (Shaw and Suess, 2003; http://structure.harvard.edu/cvm-h). This model includes the tomographic updates of Tape et al. (2009) within the background crustal structure, as well as the Boore-Joyner generic rock profiles in the shallow (upper 300 m), non-basin portions of the model.

Figure 3 shows shear wave velocity cross sections through the three seismic velocity models taken along profile A-A' as indicated in Fig. 2. Profile A-A' crosses near the deepest part of the basin where the sediment thickness is about 1.6 km. Both the Graves (2008) and CVM-S4 models use the Anderson et al (2000) basement surface to define the San Bernardino basin. The CVM-H11.1.0 does not have an explicit San Bernardino basin structure. For the Graves (2008) model, sediment shear wave velocities range from 250 m/s at the surface to about 1200 m/s in the deep basin. The background structure in this model ranges from 700 m/s at the surface to about 2500 m/s at 2 m depth. Currently, there is little direct information regarding the velocity structure of the deep basin. The values used by Graves (2008) are based on limited P-wave velocity estimates (Hadley and Combs, 1974; Stephenson et al., 2002), as well as subsequent trial-and-error adjustment to improve the fit to the ground motion data. The CVM-S4 model has similar shear wave velocities to Graves (2008) in the near surface of the basin sediments; however, the velocities increase more strongly with depth reaching a maximum of about 1800 m/s in the deepest portion of the basin. Additionally, the background velocity structure of the CVM-S4 model has much higher velocities in the upper few kilometers with shear wave velocities generally above 3000 m/s right up to the ground surface. While the CVM-H11.1.0 model does not have an explicit definition of the San Bernardino basin structure, the expression of the basin is evident in the cross section shown in Fig. 3 and results from the tomographic updates (Tape et al. 2009) included in this model. The background velocities in the CVM-H11.1.0 model lie between the values of Graves (2008) and CVM-S4. Current work is underway to include the Anderson et al. (2000) basement surface in the next release of the CVM-H model.

GROUND MOTION SIMULATIONS

I calculate the ground motions using a visco-elastic 3D finite-difference procedure (Graves, 1996) with attenuation modeled using coarse-grain operators (Day and Bradley, 2001; Graves and Day, 2003). The grid spacing is set at 0.08 km, which coupled with the minimum shear velocity threshold of 400 m/s yields a reliable bandwidth resolution of $f < 1$ Hz within the lowest velocity regions of the simulation model. Attenuation is modeled with $Q_s = 50\ V_s$ (V_s in km/s) and $Q_p = 2\ Q_s$. The simulations were run on the HPCC

Linux Cluster at USC.

The Big Bear Lake earthquake is modeled as a point double-couple source. The mechanism of the event was originally determined using regional waveform data from the Terrascope network and an automated inversion procedure (Zhu and Helmberger, 1996). Using a trial and error procedure, I adjusted the original mechanism slightly in order to improve the waveform fit at the nearby strong motion sites (original strike = 203^o and original rake = 0^o). The moment magnitude of the event is 4.63, the source depth is 7.5 km and the mechanism is primarily strike-slip. Table 1 lists the event information used in the simulation. The source time function is a cosine bell with a duration of 0.6 sec, which is effectively a delta function in the target bandwidth of the simulations ($f < 1$ Hz).

As a first step in the modeling procedure I compare the simulated and recorded waveforms at several sites surrounding the basin region. This was done to confirm the accuracy of the source description and to ensure that the wave field propagating into the basin region is modeled properly. Figure 4 compares recorded and simulated three-component ground velocity waveforms for eight sites surrounding the basin region. These sites are plotted with increasing epicentral distance from a minimum of 3.7 km at **BBR** to a maximum of 51.9 km at **RVR**. The data for the N-S component at **BBR** was not usable due to baseline contamination of the original time history. Both data and synthetics have been filtered at $f < 0.3$ Hz using a fourth-order, zero-phase butterworth operator. All of the data are plotted with respect to absolute time. For most of these sites the waveform and amplitude agreement between the simulated and observed traces is very good, indicating that the source description and background velocity structure are suitable for this bandwidth.

Figure 5 compares profiles of recorded and simulated horizontal ground velocities for a number of the sites located inside the San Bernardino basin region. Both sets of time histories have been rotated into radial and tangential components relative to the epicenter, and have been low pass filtered at $f < 0.3$ Hz. The order of the sites plotted in Fig. 5 is the same as in Fig. 2, although I have not included the CSMIP sites in Fig. 5 because the filter corner of the original data is outside the useable bandwidth of this comparison.

For most of the sites in Fig. 5, the simulated motions for the Graves (2008) model match the amplitude and waveform of the recorded motions reasonably well. As noted earlier, the recorded motions at the basin sites exhibit more waveform complexity and longer durations relative to sites north and south of the basin. The Graves (2008) simulation reproduces nicely the motions at sites in the northern basin (**np5162**, **np5337**, **np5373**) and in the south-central basin (**np129**, **np5328**, **np5431**), both in terms of peak amplitude and duration. The amplitudes of the radial motions are matched quite well, whereas the simulation tends to overpredict the amplitudes of the tangential motions at the deep basin sites. The longest observed durations are for the group of sites in the mid-central portion of the basin (**np5339**, **CLT**, **np5329**). Although the simulation matches the peak motions at these sites, it generally underpredicts the total durations. This suggests that the Graves (2008) basin structure may need some refinement in the mid-central basin region. In particular, expanding the deep basin trough toward the northeast would increase the potential for trapping surface wave energy in the vicinity of these sites.

The motions simulated with the CVM-S4 model also show strong basin response effects in the $f < 0.3$ Hz bandwidth, although the fit to the observed waveforms is generally not as good as with the Graves (2008) model. The CVM-S4 motions tend to arrive somewhat earlier than the observed motions, and this model has a strong overprediction of the tangential motions within the deep basin. These features are consistent with the faster shear velocities of the background structure of CVM-S4, which not only provides a faster travel path from the source, but also a stronger impedance contrast with the basin sediments, which tends to amplify the basin motions.

As expected, the motions simulated with the CVM-H11.1.0 model do not exhibit a strong basin response. However, these motions do match the timing and amplitude of the initial arrivals quite well with a generally better match to the tangential component waveforms than the radial. In some respects, this should not be a surprising result since these waveform data were used in the tomographic modeling by Tape et al. (2009), which is incorporated in CVM-H11.1.0.

Figure 6 plots profiles of the ground velocities simulated with the three models for the pass band $f < 1$ Hz. For this pass band, I also include the response simulated for the CSMIP sites. The simulated motions for the Graves (2008) and CVM-S4 models reproduce many of the characteristics seen in the observed motions, as shown in Fig. 2. These characteristics include relatively simple waveforms north of the basin, increased amplitudes and extended durations within the basin, and reduction of amplitudes and decreased waveform complexity south of the basin. Despite this general agreement, the simulated motions for the Graves (2008) model tend to underpredict the overall durations of the observed motions, and those for the CVM-S4 model tend to overpredict the observed amplitudes. These features are seen both for sites inside (e.g., **np5329**) as well as outside (e.g., **RVR**) the basin. This suggests that these 3D models do not contain enough structural complexity at the shorter length scales to adequately represent the real structure.

The $f < 1$ Hz motions for the CVM-H11.1.0 simulation show relatively simple waveforms across the profile of sites displayed in Fig. 6. While there is some amplification of the response within the basin due to the lower near surface velocities provided by the V_{s30} calibration in this model (see Fig. 3), the motions are dominated by the primary S-wave arrivals. In addition, the tangential motions

are about 2 – 4 times larger than the radial motions as a result of the radiation pattern from the source. Due to scattering within the basin, the recorded motions show nearly the same peak amplitude level for both radial and tangential components, typically from arrivals much later in the record than the direct S-wave (see Fig. 2).

Figure 7 compares the observed PGV levels across the Los Angeles region with those simulated for models CVM-S4 and CVM-H11.1.0 for the bandwidths of f < 0.3 Hz and f < 1.0 Hz. In both bandwidths, the observed motions show relatively large amplitudes to the south and west of the epicenter in the near source region. The motions decrease just north of the San Bernardino basin showing relatively smaller amplitudes (near lon=-117.25^o, lat=34.20^o), with an increase in amplitudes seen over the deeper portion of the basin (near lon=-117.25^o, lat=34.10^o). Further to the west, the observed motions show pockets of amplification at the juncture of the San Gabriel and Los Angeles basins (near lon=-118^o, lat=34^o), along the NW-SE axis of the Los Angeles basin, and in the northwestern San Fernando basin region (near lon=-118.50^o, lat=34.25^o). These features are match to varying degrees of success in the simulations for both seismic velocity models. The notable exceptions are the underprediction of amplification in the San Bernardino basin and San Gabriel / Los Angeles basin juncture in CVM-H11.1.0, and the overprediction of amplification in the Chino basin in CVM-S4.

CONCLUSIONS

The comparison between the simulated ground motions for the San Bernardino basin region indicates that the Graves (2008) model produces a better fit to the observations than that obtained with the CVM-S4 and CVM-H11.1.0 models. The CVM-S4 model provides a generally good match to the observed motions, but noticeably overpredicts the amplitude of the waveforms in the central portion of the basin. I suspect that this is caused by the relatively high shear wave velocities in the background portion of CVM-S4. The CVM-H11.1.0 model does not have an explicit representation of the San Bernardino basin, although there is a region of lower shear wave velocity present in the tomographic background portion of this model, which is probably a subtle expression of this basin structure. Consequently, the CVM-H11.1.0 model is not able to reproduce the observed basin response in the San Bernardino region. However, this model is currently being revised to incorporate the Anderson et al. (2000) basement structure, and subsequent analysis will examine how the updated model compares with the observed response.

Examining the response across the larger scale Los Angeles basin region, both CVMs do reasonable well in matching the observed pattern of amplification in the central Los Angeles and northwestern San Fernando basins. The simulation for CVM-S4 tends to overpredict the response in the Chino basin and the channeling of energy from the San Gabriel to Los Angeles basins, particularly at higher frequencies. The simulation for CVM-H11.1.0 underpredicts the response at the juncture of the San Gabriel and Los Angeles basins. This result may be improved once the San Bernardino basin structure is added to CVM-H since this would create a series of interconnected basins extending from the source region into the Los Angeles region (San Bernardino – Chino – San Gabriel – Los Angeles).

ACKNOWLEDGEMENTS

The large-scale 3D finite difference simulations were run at USC's Center for High Performance Computing and Communications (http://www.usc.edu/hpcc) under an agreement with the SCEC Community Modeling Environment project. All figures in the paper were generated using GMT version 4.2.1 (www.soest.hawaii.edu/gmt; Wessel and Smith, 1998).

REFERENCES

Anderson, M. L., C. W. Roberts, and R. C. Jachens (2000). Principal facts for gravity stations in the vicinity of San Bernardino, southern California, *U.S. Geol. Surv. Open-File Rept. 00-193*, 32 pp.

Day, S. M., and C. R. Bradley (2001). Memory efficient simulation of anelastic wave propagation, *Bull. Seism. Soc. Am.* **91**, 520–531.

Frankel, A. (1994). Dense array recordings in the San Bernardino valley of Landers-Big Bear aftershocks: basin surface waves, Moho reflections, and three-dimensional simulations, *Bull. Seism. Soc. Am.,* **84**, 613–624.

Graves, R. W. (1996). Simulating seismic wave propagation in 3D elastic media using staggered grid finite differences, *Bull. Seism. Soc. Am.,* **86**, 1091–1106.

Graves, R. W. (2008). The seismic response of the San Bernardino basin region during the 2001 Big Bear Lake earthquake, *Bull. Seismol. Soc. Am.* **98**, 241-252.

Graves, R. W. and Steven M. Day (2003). Stability and accuracy analysis of coarse-grain viscoelastic simulations, *Bull. Seism. Soc. Am.,* **93**, 283-300.

Hadley, D. and J. Combs (1974). Microearthquake distribution and mechanisms of faulting in the Fontana-San Bernardino area of southern California, *Bull. Seism. Soc. Am.*, **64**, 1477-1499.

Kohler, M., H. Magistrale, and R. Clayton (2003) Mantle heterogeneities and the SCEC three-dimensional seismic velocity model version 3, *Bull. Seism. Soc. Am.,* **93**, 757-774.

Magistrale, H., S. Day, R. Clayton, and R. Graves (2000) The SCEC southern California reference three-dimensional seismic velocity model version 2, *Bull. Seism. Soc. Am.,* **90** (6B), S65-S76.

Stephenson, W. J., J. K. Odum, R. A. Williams and M. L. Anderson (2002). Delineation of faulting and basin geometry along a seismic reflection transect in urbanized San Bernardino valley, California, *Bull. Seism. Soc. Am.*, **92**, 2504-2520.

Suess, M. P., and J. H. Shaw (2003). P wave seismic velocity structure derived from sonic logs and industry reflection data in the Los Angeles basin, California, *J. Geophys. Res.*, 108 (B3), 2170, doi: 10.1029/2001JB001628.

Tape, C., Q. Liu, A. Maggi, and J. Tromp, 2009, Adjoint tomography of the southern California crust, *Science*, **325**, 988-992.

Wessel, P., and W. H. F. Smith (1998). New, improved version of Generic Mapping Tools released, *EOS Trans. Amer. Geophys. U.*, **79** (47), pp. 579.

Wills, C. J., M. Petersen, W. A. Bryant, M. Reichle, G. J. Saucedo, S. Tan, G. Taylor, and J. Treiman (2000). A Site-Conditions Map for California Based on Geology and Shear-Wave Velocity, *Bull. Seism. Soc. Am.*, **90**, S187-S208.

Zhu, L. and D. V. Helmberger (1996). Advancement in source estimation techniques using broadband regional seismograms, *Bull. Seism. Soc. Am.*, **86**, 1634-1641.

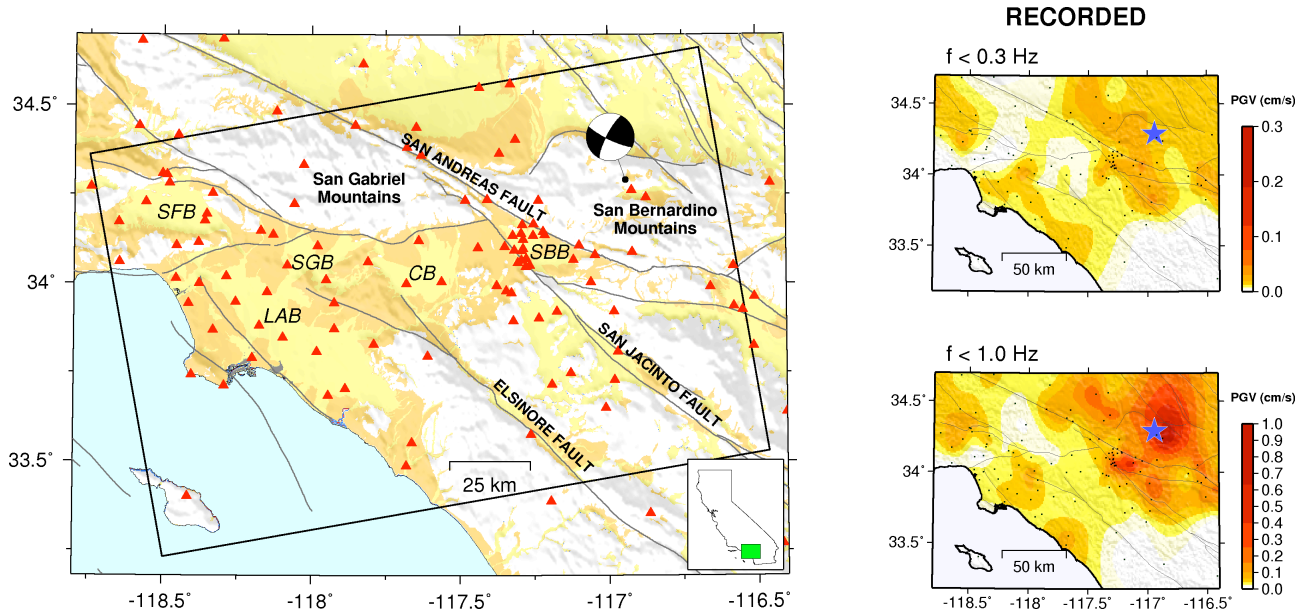

Fig 1. Left shows map view of southern California region covered by the 3D simulation models. Red triangles are sites of strong motion and broadband instruments that recorded the 02/10/2001 Mw 4.6 Big Bear Lake event. Epicenter of event denoted by black circle. Basin regions are: CB – Chino basin, SGB – San Gabriel basin, LAB – Los Angeles basin, SFB – San Fernando basin. Right shows peak ground velocity contour maps derived from observations filtered at f < 0.3 Hz (top) and f < 1.0 Hz (bottom).

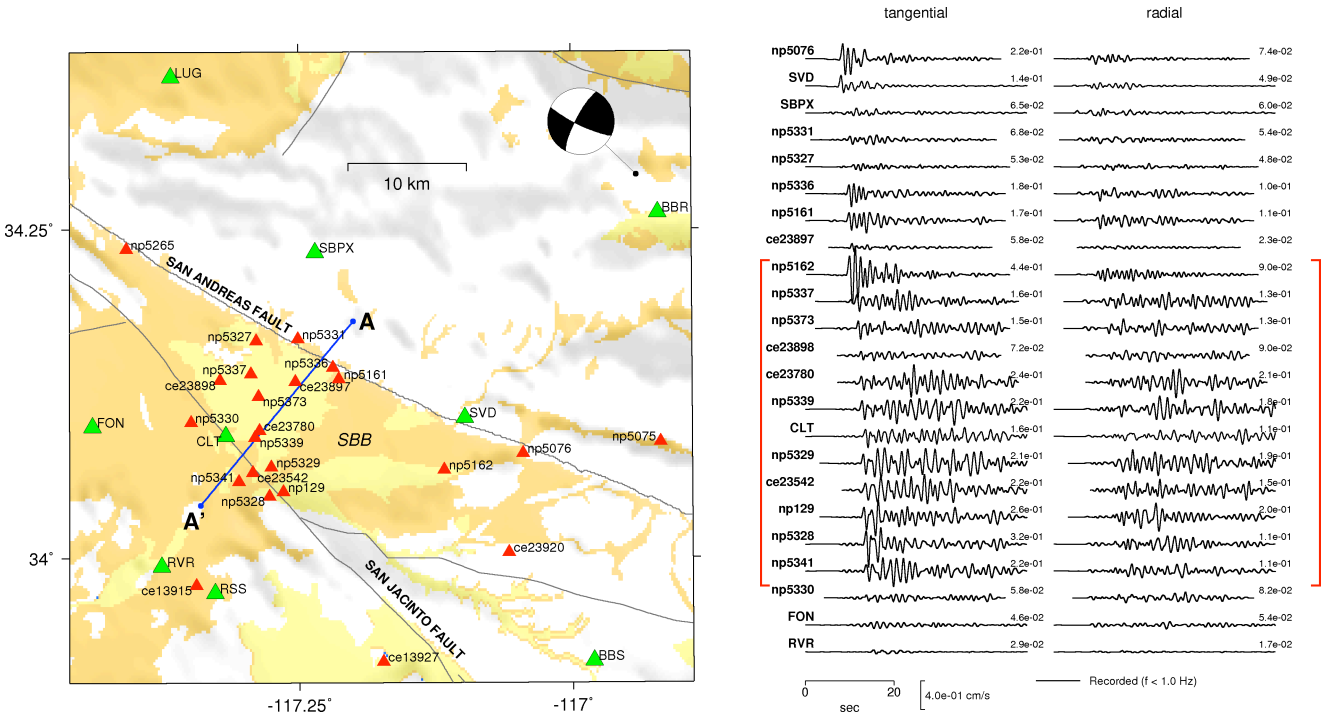

Fig 2. Left shows map view of San Bernardino basin region showing Big Bear Lake event epicenter (black circle), strong motion (red triangles) and broadband (green triangles) instrument sites and location of cross section A-A'. Right shows profiles of recorded tangential and radial component ground velocity for sites in San Bernardino basin region. Waveforms are filtered at f < 1.0 Hz. Red brackets indicate sites in the central portion of the basin.

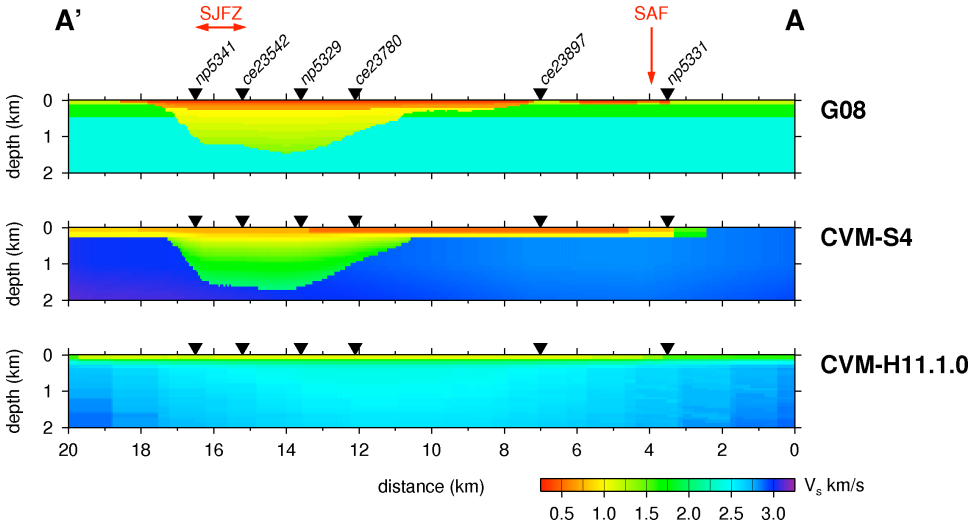

Fig 3. Cross sections of shear wave velocity along profile A-A' for the 3 velocity models considered in this study.

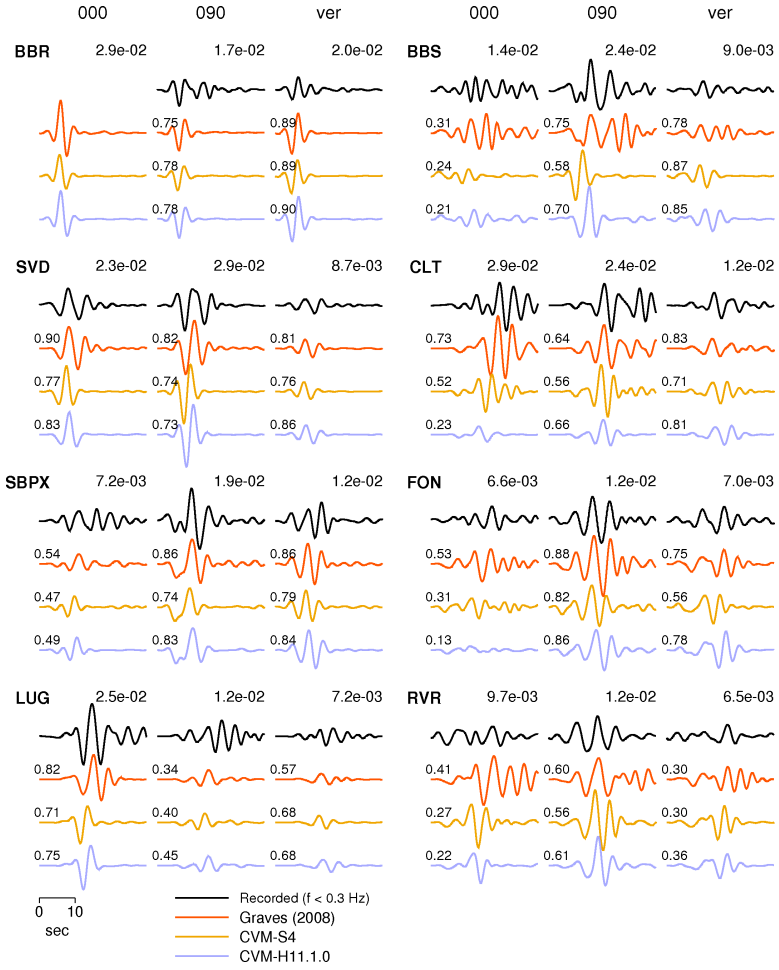

Fig 4. Comparison of recorded (black traces) and simulated (colored traces) ground velocities for sites surrounding the basin region. All waveforms are filtered at f < 0.3 Hz. All waveforms at each station are scaled to same peak amplitude. Largest peak amplitude for each component is listed above each set of traces. Numbers to left of each simulated trace indicate the waveform cross-correlation coefficient with respect to the recorded motion.

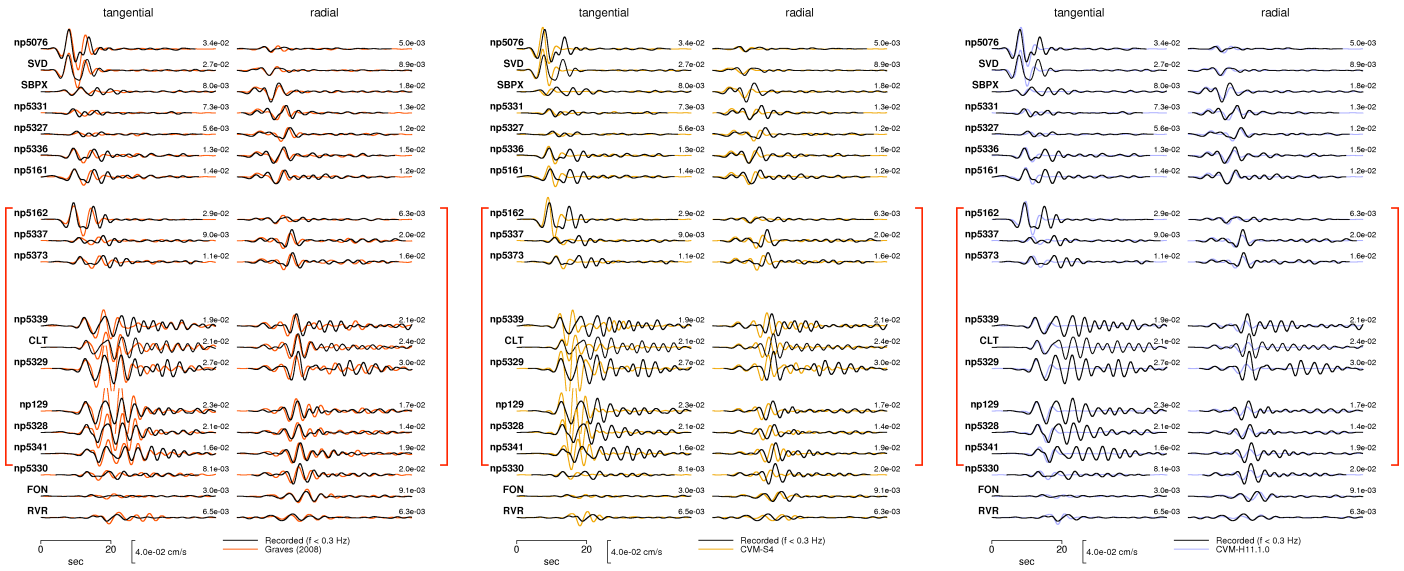

Fig. 5. Comparison of recorded (black traces) and simulated (colored traces) ground motions for San Bernardino basin region sites. All waveforms are filtered at f < 0.3 Hz. Left panel: Graves (2008), middle panel: CVM-S4, right panel: CVM-H11.1.0.

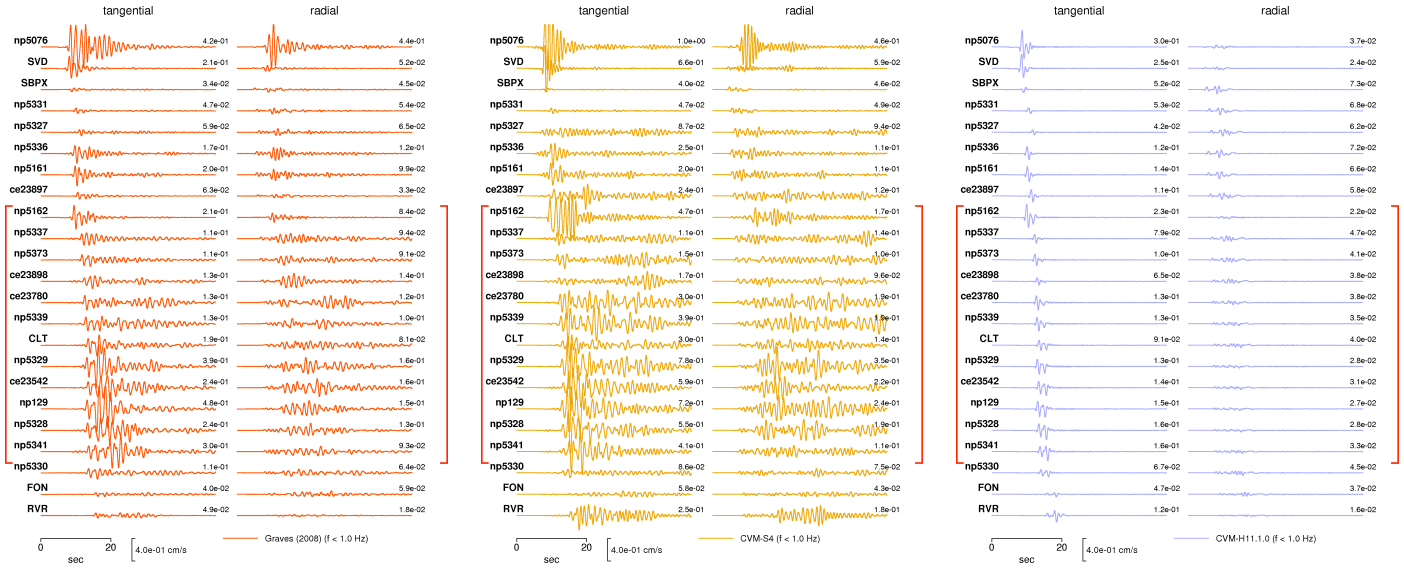

Fig. 6. Simulated ground motions for San Bernardino basin region sites filtered at f < 1.0 Hz. Left panel: Graves (2008), middle panel: CVM-S4, right panel: CVM-H11.1.0. Compare with recorded motions shown in Fig. 2.

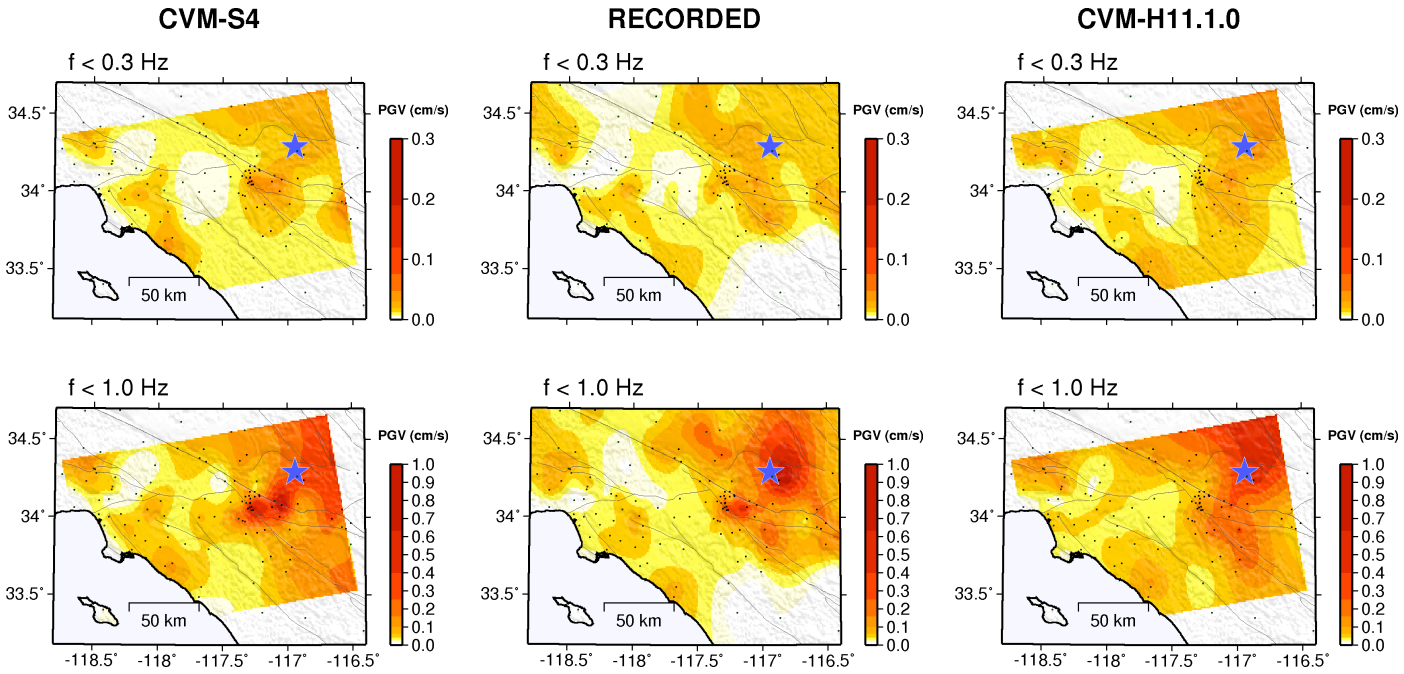

Fig. 7. Comparison of observed (middle column) and simulated left and right columns) peak ground velocity throughout the Los Angeles region for the Big Bear Lake event. Epicenter indicated by star and black circles indicate locations of recording sites used to derive contours. Top row are filtered at f < 0.3 Hz and bottom row are filtered at f < 1.0 Hz. Left panels: CVM-S4, right panels: CVM-H11.1.0.